Journal of Applied Mechanics and Technical Physics, Vol. 40, No. 4, 1999

HEAT TRANSFER CHARACTERISTICS IN FLOW AROUND A SPHERICALLY BLUNTED CONE AT INCIDENCE AND GAS INJECTION FROM A BLUNTED SURFACE

V. I. Zinchenko and A. S. Yakimov[1]

UDC 536.24

New methods of controlling thermal regimes in a high-enthalpy spatial flow around a body are considered. They are related to gas injection from the blunted surface and heat overflow in the material of the shell. The effect of injection is analyzed for different thermal conductivities. It is shown that highly heat-conducting materials can be successfully used to decrease the maximum temperatures at the windward side due to intense heat removal to the region of a porous spherical bluntness.

For stationary heating regimes [1], heat overflow in the material of a body located in a high-enthalpy flow is an effective method of decreasing the temperature in regions with the maximum thermal loads. The analysis of the characteristics of nonstationary heat transfer for different boundary-layer flow regimes [2] showed that the injection of a cooling gas is a reliable method of thermal protection of a structure from overheating. This injection involves an attenuation of the heat flux supplied to the surface and heat removal during gas filtration in the pores. In contrast to axisymmetric heating [1, 2], the difference in heat fluxes on the leeward and windward sides of a body at incidence can be quite significant [3], which causes heat overflow in the circumferential direction. Zinchenko et al. [3] studied the influence of thermophysical properties of a number of materials on the temperature fields of the conical part of the body and concluded that it is reasonable to use highly heat-conducting coatings, which ensure intense heat removal to the region of a porous spherical bluntness. The problem of heat transfer in the region of the porous bluntness was not considered in that paper, and simplified boundary conditions were used at the interface between the spherical and conical parts of the body.

In the present paper, we use a complete formulation of the problem in a compound body. The boundary conditions in mathematical modeling of heat transfer correspond to setting convective heat fluxes from the side of the gaseous phase for a spatial supersonic flow around a spherically blunted cone with account of the effect of injection from the surface of the porous bluntness.

1. Formulation of the Problem. With account of the assumption of one-dimensionality of the process of filtration of the gas injected normally to the body surface and the one-temperature character of the porous medium, the conservation equation for energy in the conventional coordinate system related with the body centerline for a permeable spherical shell of a compound body (Fig. 1) is written in the following form:

$$c_\Sigma \frac{\partial T_1}{\partial t} - c_g \frac{(\rho v)_w r_{1w}}{H r_1} \frac{\partial T_1}{\partial n_1} = \frac{1}{H r_1}\left[\frac{\partial}{\partial n_1}\left(H r_1 \lambda_\Sigma \frac{\partial T_1}{\partial n_1}\right) + \frac{\partial}{\partial s}\left(\frac{r_1 \lambda_\Sigma}{H}\frac{\partial T_1}{\partial s}\right) + \frac{\partial}{\partial \eta}\left(\frac{H}{r_1}\lambda_\Sigma \frac{\partial T_1}{\partial \eta}\right)\right], \tag{1.1}$$

$$0 < s < s_A, \quad 0 < n_1 < L, \quad 0 < \eta < \pi, \quad H = \frac{R_N - n_1}{R_N}, \quad r_1 = (R_N - n_1)\sin\bar{s}, \quad \bar{s} = \frac{s}{R_N}.$$

Tomsk State University, Tomsk 634050. [1]Tomsk University of Control Systems and Radioelectronics, Tomsk 634050. Translated from Prikladnaya Mekhanika i Tekhnicheskaya Fizika, Vol. 40, No. 4, pp. 162–169, July–August, 1999. Original article submitted April 28, 1997.

0021-8944/99/4004-0697 $22.00

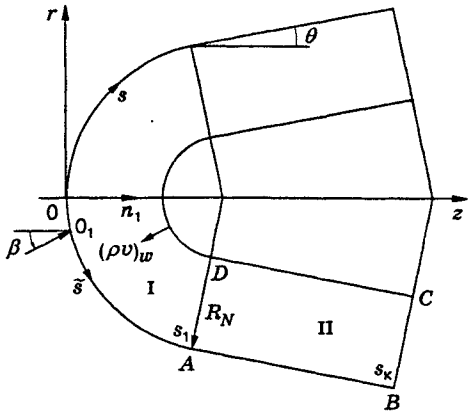

Fig. 1

For the conical part of the shell (region II in Fig. 1), the heat-conductivity equation is

$$(r\rho c_p)_2\frac{\partial T_2}{\partial t} = \frac{\partial}{\partial n_1}\Big(r_2\lambda_2\frac{\partial T_2}{\partial n_1}\Big) + \frac{\partial}{\partial s}\Big(r_2\lambda_2\frac{\partial T_2}{\partial s}\Big) + \frac{1}{r_2}\frac{\partial}{\partial \eta}\Big(\lambda_2\frac{\partial T_2}{\partial \eta}\Big),$$
$$s_A < s < s_B, \quad r_2 = (R_N - n_1)\cos\theta + (s - s_A)\sin\theta. \tag{1.2}$$

System (1.1), (1.2) should be solved with the initial and boundary conditions

$$T_i\big|_{t=0} = T_{\text{in}} \qquad (i = 1, 2). \tag{1.3}$$

We have

$$q_w - \varepsilon_1\sigma T_{1w}^4 = -\lambda_\Sigma\frac{\partial T_1}{\partial n_1}\Big|_w \tag{1.4}$$

on the external heated boundary of the gas flow/body interface $0A$ in the region of spherical bluntness (region I in Fig. 1) and

$$q_w - \varepsilon_2\sigma T_{2w}^4 = -\lambda_2\frac{\partial T_2}{\partial n_1}\Big|_w \tag{1.5}$$

on the external surface of the nonpermeable cone. Heat transfer on the internal surface of the permeable region I is specified using the Newton law with regard for injection:

$$\lambda_\Sigma\Big(\frac{\partial T_1}{\partial n_1}\Big)\Big|_L = \frac{r_{1w}c_g(\rho v)_w}{(Hr_1)_L}\Big(T_{\text{in}} - T\big|_L\Big). \tag{1.6}$$

On the junction ring AD, we have the perfect contact conditions

$$\frac{\lambda_\Sigma}{H}\frac{\partial T_1}{\partial s} = \lambda_2\frac{\partial T_2}{\partial s}, \qquad T_1 = T_2. \tag{1.7}$$

The conditions of heat insulation are imposed on the lines DC and BC:

$$\frac{\partial T_2}{\partial n_1} = 0, \qquad \frac{\partial T_2}{\partial s} = 0. \tag{1.8}$$

For heat transfer with a plane of symmetry, we can write

$$\Big(\frac{\partial T_i}{\partial \eta}\Big)\Big|_{\eta=0} = \Big(\frac{\partial T_i}{\partial \eta}\Big)\Big|_{\eta=\pi} = 0 \qquad (i = 1, 2). \tag{1.9}$$

To prescribe the heat flux from the gaseous phase q_w, we use the formulas derived by Zemlyanskii and Stepanov [4] for a spatial case of laminar and turbulent flow regimes in the boundary layer. To decrease the heat flux in the case of injection of a cooling gas whose composition coincides with the incoming air stream, we

use the formulas from [5]. For a laminar flow regime in the boundary layer, we obtain the following equation for the porous spherical part in the coordinate system fitted to the stagnation point 0_1:

$$q_w = \left(\frac{\alpha}{c_p}\right)^0\left[1 - \frac{0.6(\rho v)_w}{(\alpha/c_p)^0}\right](h_r - h_w), \qquad \left(\frac{\alpha}{c_p}\right)^0 = \frac{1.05V_\infty^{1.08}[0.55 + 0.45\cos(2\tilde{s})]}{(R_N/\rho_\infty)^{0.5}},$$

$$h_r = h_{e0}\left[\left(\frac{p_e}{p_{e0}}\right)^{(\gamma-1)/\gamma} + \left(\frac{u_e}{v_m}\right)^2 \mathrm{Pr}^{0.5}\right], \qquad \frac{u_e}{v_m} = \left[1 - \left(\frac{p_e}{p_{e0}}\right)^{(\gamma-1)/\gamma}\right]^{0.5}, \qquad 0_1 \leqslant \tilde{s} \leqslant \tilde{s}_*,$$

$$h_w = b_1 T_w + b_2 T_w^2/2, \qquad \tilde{s} = \arccos(\cos\bar{s}\cos\beta + \sin\bar{s}\sin\beta\cos\eta).$$

For a turbulent boundary-layer flow regime, we have

$$q_w = \left(\frac{\alpha}{c_p}\right)^0 \exp\left[-\frac{0.37(\rho v)_w}{(\alpha/c_p)^0}\right](h_r - h_w), \quad \left(\frac{\alpha}{c_p}\right)^0 = \frac{16.4V_\infty^{1.25}\rho_\infty^{0.8}}{R_N^{0.2}(1 + h_w/h_{e0})^{2/3}}(3.75\sin\tilde{s} - 3.5\sin^2\tilde{s}),$$

$$h_r = h_{e0}\left[\left(\frac{p_e}{p_{e0}}\right)^{(\gamma-1)/\gamma} + \left(\frac{u_e}{v_m}\right)^2 \mathrm{Pr}^{1/3}\right], \qquad \tilde{s}_* < \tilde{s} \leqslant \tilde{s}_1.$$

To evaluate the effect of injection on the heat flux in the screening region, we use the data [6] and formulas [3] obtained by processing of the results of exact numerical calculations of a spatial boundary layer and a viscous shock layer [7, 8]:

$$q_w = \left(\frac{\alpha}{c_p}\right)^0 (1 - k_1 b^{k_2})(h_r - h_w), \qquad \left(\frac{\alpha}{c_p}\right)^0 = \frac{16.4V_\infty^{1.25}\rho_\infty^{0.8}2.2(p_e/p_{e0})u_e/v_m}{R_N^{0.2}(1 + h_w/h_{e0})^{2/3}k^{0.4}\bar{r}_{2w}^{0.2}},$$

$$k = (\gamma - 1 + 2/\mathrm{M}_\infty^2)/(\gamma + 1), \qquad \tilde{s}_A \leqslant \tilde{s} \leqslant \tilde{s}_B.$$

For the flow rate of the cooling gas

$$(\rho v)_w(\tilde{s}) = (\rho v)_w(0_1)(1 + a\sin^2\tilde{s}), \tag{1.10}$$

we have

$$b = \frac{2(\rho v)_w(0_1)\{1 - \cos\tilde{s}_1 + a[2/3 - \cos\tilde{s}_1 + (1/3)\cos^3\tilde{s}_1]\}}{(\alpha/c_p)^0(\bar{s} - \bar{s}_1)[2\cos\theta + (\bar{s} - \bar{s}_1)\sin\theta]},$$

$$\cos\tilde{s}_1 = \cos\bar{s}_1\cos\beta + \sin\bar{s}_1\sin\beta\cos\eta, \qquad \bar{s}_1 = \bar{s}_A = \pi/2 - \theta.$$

Here and below, t is the time, r and z are the transverse and longitudinal components of the cylindrical coordinate system, n_1, s, and η are the components of the conventional coordinate system, T, p, and ρ are the temperature, pressure, and true density, $(\rho v)_w$ is the flow rate of the cooling gas, c_p and λ are the heat capacity and thermal conductivity, h is the enthalpy, r_1, r_2, and H are the Lamé coefficients, φ and R_N are the porosity and the radius of the spherical bluntness, σ is the Stefan–Boltzmann constant, ε_i $(i = 1, 2)$ is the emissive power of the surface of the exposed material, $\tilde{s}_*$ is the coordinate of the point of loss of stability in the coordinate system with the origin at the stagnation point, β and θ are the angle of attack and conicity, Re and Pr are the Reynolds and Prandtl numbers, L is the shell thickness, V_∞, ρ_∞, and M_∞ are the free-stream velocity, density, and Mach number, and μ is the gas-flow viscosity. The subscripts $e0$ and w correspond to the conditions at the external edge of the boundary layer at the stagnation point and at the interface between the gaseous and solid phases, the subscripts 1 and 2 correspond to the number of the region of the compound shell, g to the gas characteristics in a porous medium, the subscripts "in" and the asterisk to the initial and characteristic parameters, the bar indicates dimensionless quantities, the superscript 0 marks the parameters α/c_p and q_w in the absence of injection, L corresponds to the quantities at the internal surface of the shell, Σ to the total values of the quantities, "e" to the equilibrium radiation temperature, and "f" to the final values of the quantities.

2. Calculation Method and Initial Data. The boundary-value problem (1.1)–(1.9) was solved numerically using implicit difference equations on the basis of a locally one-dimensional splitting scheme [9]. Since the shock-capturing method is used for curves $BA0$ due to the conjugation condition (1.7), the

circumferential coordinate η varies within $0 \leqslant \eta \leqslant \pi$. A $11 \times 41 \times 11$ grid was used and the time of solution of the basic (three-dimensional) variant until reaching a steady distribution of the body temperature was 15 min on a IBM-486 computer. The solution differed by no more than 1.5 % if the number of nodes in the spatial grid was increased by a factor of two. The numerical solution obtained with an automatic choice of the time step from the condition of prescribed accuracy differed from the calculation with a constant time step only by 0.5 %; therefore, to save computer time, the numerical results were obtained at a constant time step.

The flow around a spherically blunted cone occurred in a turbulent flow regime in the boundary layer [$\mathrm{Re} = \rho_{e0} R_N (2h_{e0})^{0.5}/\mu_{e0} \approx 0.7 \cdot 10^6$ is the Reynolds number found from the stagnation parameters]. The pressure distribution over the body surface normalized to the stagnation pressure $\bar{p} = p_e/p_{e0}$ was found from solving a spatial gas-dynamic problem [10]. The thermophysical constants of copper were borrowed from [5], air was chosen as the cooling gas [11], and the main results were obtained for the following parameters:

$$
\begin{aligned}
&c_\Sigma = c_{p_1}\rho_1(1-\varphi) + c_g\rho_g\varphi, && \lambda_\Sigma = \lambda_1(1-\varphi) + \lambda_g\varphi,\\
&c_g = b_1 + b_2 T, && h_{e0} = h_\infty[1 + 0.5(\gamma-1)\mathrm{M}_\infty^2],\\
&T_{\text{in}} = T_\infty = 300\ \mathrm{K}, && c_{p\infty} = 10^3\ \mathrm{J/(kg \cdot K)},\\
&\lambda_i = 386\ \mathrm{W/(m \cdot K)}, && \rho_g = 1.3\ \mathrm{kg/m^3},\\
&\rho_i = 8950\ \mathrm{kg/m^3}, && \lambda_g = 0.026\ \mathrm{W/(m \cdot K)},\\
&c_{p_i} = 370\ \mathrm{J/(kg \cdot K)}, && L = 5 \cdot 10^{-3}\ \mathrm{m},\\
&\varepsilon_i = 0.85,\ i = 1, 2, && R_N = 1.85 \cdot 10^{-2}\ \mathrm{m},\\
&\rho_\infty = 0.0208\ \mathrm{sec^2 \cdot kgf/m^4}, && V_\infty = 2.08\ \mathrm{km/sec},\\
&\beta = 20^\circ,\ \theta = 5^\circ, && b_1 = 965.5,\ b_2 = 0.147,\\
&\varphi = 0.34,\ \gamma = 1.4, && \mathrm{M}_\infty = 6,\ \mathrm{Pr} = 0.72,\\
&k_1 = 0.285, && k_2 = 0.165,\ a = 3.
\end{aligned}
$$

To control the numerical solution of the problem, we used an analytical solution for stationary heat transfer in the form of an integral conservation law. Then the surface temperature satisfies the relationship

$$
\int_0^\pi \left\{ \int_0^{s_1} r_{1w}[q_w - \varepsilon_1\sigma T_w^4 + c_g(\rho v)_w(T_{\text{in}} - T_w)]\, ds \int_{s_1}^{s_f} r_{2w}(q_w - \varepsilon_2\sigma T_w^4)\, ds \right\} d\eta = 0, \tag{2.1}
$$

which is obtained by integration of the initial boundary-value problem in the steady case. For $\lambda_1 \to \infty$ and $\lambda_2 \to \infty$, the temperature field in the material of the body becomes uniform and the value of the desired temperature is in good agreement with the calculation results obtained by solving the nonlinear algebraic equation

$$
\begin{aligned}
&(h_{e0} - c_g T_w) \int_0^\pi \left[\int_0^{s_1} r_{1w} \left(\frac{\tilde{\alpha}}{c_p}\right) ds + \int_{s_1}^{s_f} \left(\frac{\tilde{\alpha}}{c_p}\right) r_{2w}\, ds + c_g(T_{\text{in}} - T_w) \int_0^{s_1} r_{1w}(\rho v)_w\, ds \right] d\eta\\
&\quad = \pi\sigma T_w^4 \left(\varepsilon_1 \int_0^{s_1} r_{1w}\, ds + \varepsilon_2 \int_{s_1}^{s_f} r_{2w}\, ds \right), \qquad \left(\frac{\tilde{\alpha}}{c_p}\right) = \left(\frac{\alpha}{c_p}\right) \frac{h_r - h_w}{h_{e0} - h_w},
\end{aligned} \tag{2.2}
$$

which follows from (2.1) if the heat flux formula is used in the form $q_w = (\tilde{\alpha}/c_p)(h_{e0} - c_g T_w)$, where $c_g = \mathrm{const}$.

3. Analysis of the Numerical Solution. Figure 2 shows the surface temperature T_w and convective heat flux from the gaseous phase q_w (solid curves 1–3) as functions of the coordinate $\bar{s}$ on the windward and leeward sides of the plane of symmetry for $(\rho v)_w = 0$. Curves 1–3 correspond to times $t = 0$, 10, and 200 sec (in the latter case, a steady regime of the body heating process is observed). To evaluate the effect of heat overflow in the circumferential direction, we considered the solution of a two-dimensional problem resulting from (1.1), (1.2). The results corresponding to this solution are presented by dashed curves (the dashed and solid curves 1 for q_w and T_w coincide at $t = 0$). The dot-and-dashed curve shows the distribution of the equilibrium radiation temperature T_{we} in the plane of symmetry on the windward and leeward sides, which

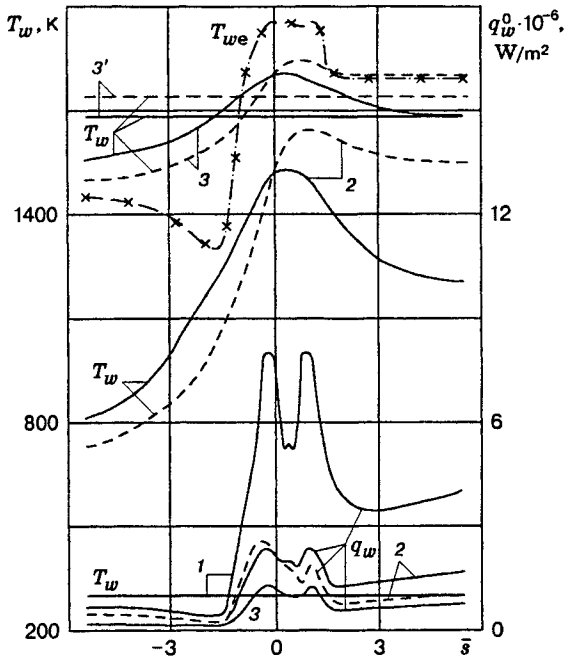

Fig. 2

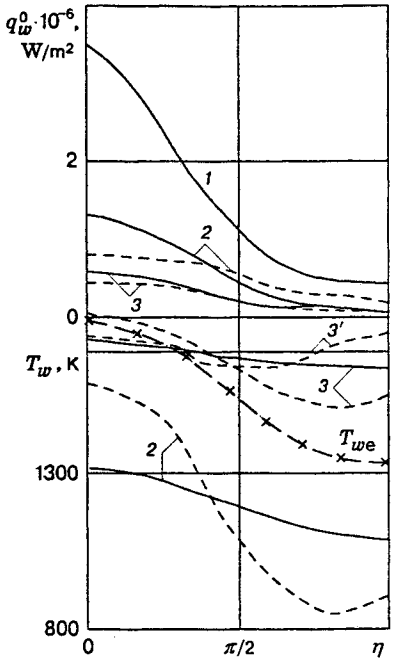

Fig. 3

was found from the condition of energy conservation on the porous and conical surfaces

$$q_w + c_g(\rho v)_w(T_{in} - T_{we}) = \varepsilon_1 \sigma T_{we}^4, \qquad q_w = \varepsilon_2 \sigma T_{we}^4 \tag{3.1}$$

and defines the maximum reachable temperature of the surface in the absence of heat overflow in the longitudinal and circumferential directions. Because of external heating, the surface temperature of the nonpermeable body increases and its highest value corresponds to the equilibrium radiation temperature in the region of the maximum heat flux for a turbulent flow regime in the boundary layer near the stagnation point. As should be expected, accounting for heat overflow gives a significant decrease in T_w for a highly heat-conducting material like copper. Neglect of heat overflow in the circumferential direction overestimates the surface temperature at the current moments of time by more than 300 K and significantly underestimates T_w on the leeward side (solid and dashed curves 2). Note also that, when the steady process is reached, the surface temperature on the leeward side is significantly higher than the equilibrium radiation temperature T_{we} because of longitudinal and circumferential overflow of heat. Along with the calculation of T_{we} from conditions (3.1), we solved the initial-boundary problem for a poorly heat-conducting material, such as asbestos cement [$\lambda_i = 0.349$ W/(m·K), $c_{p_i} = 837$ J/(kg·K), and $\rho_i = 1800$ kg/m^3, $i = 1$ and 2]. When the steady regime was reached after equalization of the temperature fields across the shell, the values of T_w coincided with T_{we} (the curve marked by crosses in Fig. 2), since the heating process for this material is one-dimensional.

The calculation results for the steady regime of the heating process for $\lambda_i \to \infty$ ($i = 1, 2$) show that the temperature profile in the exposed material becomes uniform (straight lines 3') and the values of temperature in three-dimensional heating are in good agreement with the calculation results from formula (2.2). Figure 3 (the notation is the same as in Fig. 2) shows the distributions of T_w and q_w along the circumferential coordinate on the conical part of the shell in the cross section $\bar{s} = 2.3$ close to the spherical tip. A significant difference in temperature in the three-dimensional and two-dimensional cases is observed in the most heat-loaded cross section $\eta = 0$ (~269 K) and the cross section $\eta \approx 0.8\pi$ (~258 K) at $t = 10$ sec. Nevertheless, the maximum difference in T_w for $t = 10$ sec is observed at the peripheral part of the shell for $\bar{s} = \bar{s}_B$ and $\eta = 0$ and approximately amounts to 348 K (see Fig. 2). The nonmonotonic pressure distribution $p_e = p_e(s, \eta)$ along the circumferential coordinate defines also the nonmonotonic behavior of the copper temperature for $\lambda_i \to \infty$ ($i = 1, 2$) in the two-dimensional case (dashed curve 3').

We consider the effect of the flow rate of the cooling gas from the blunted surface. Figure 4 shows

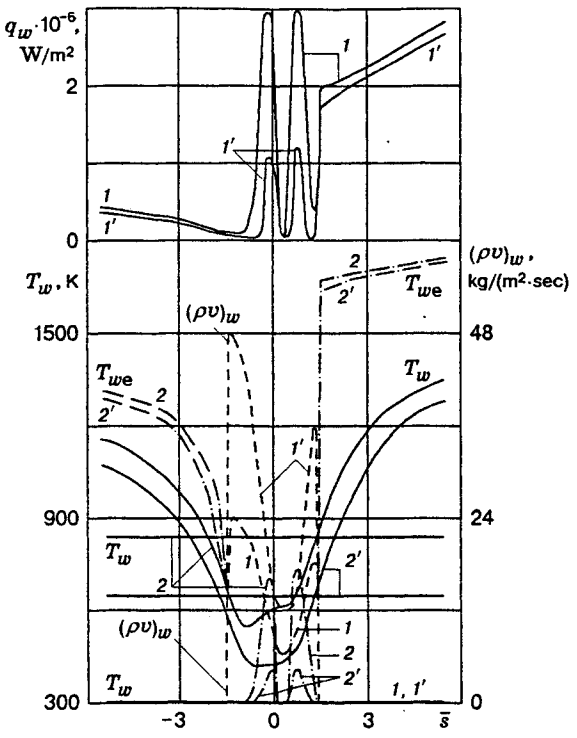

Fig. 4

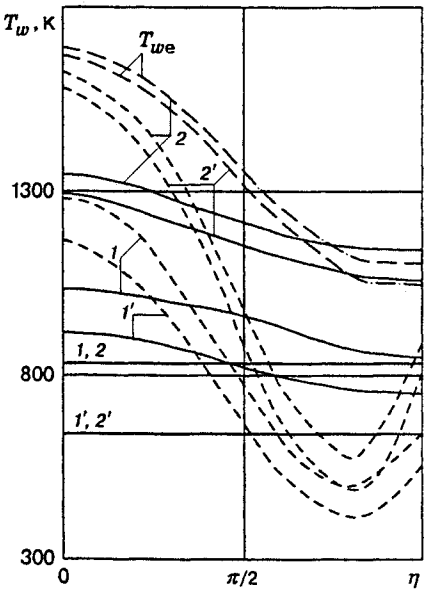

Fig. 5

the distributions of the heat fluxes q_w (solid curves 1 and 1′) and the surface temperature T_w for the initial time $t = 0$ (curves 1 and 1′) and in the steady regime of the process (solid curves 2 and 2′). Curves 1 and 2 and 1′ and 2′ were obtained for the flow rates $(\rho v)_w(0_1) = 6$ and 12 kg/(m^2·sec) at the stagnation point 0_1, respectively. The flow rate of the cooling gas defined by formula (1.10) in the vicinity of the plane of symmetry is shown by the dashed curves 1 and 1′ for $(\rho v)_w(0_1) = 6$ and 12 kg/(m^2·sec), respectively. The dot-and-dashed curves 2 and 2′ correspond to the equilibrium radiation temperature with different values of the flow rate. Straight lines 2 and 2′ correspond to the data obtained for $\lambda \to \infty$ and agree with the results obtained using formulas (2.2). The injection of a cooling gas from a porous bluntness leads to a significant decrease (by a factor of 2.5) in the maximum of q_w on the sphere and its twofold decrease on the conical part of the body (solid curves in Figs. 2 and 4). In addition, the heat is also absorbed here during gas filtration in the pores. As a result, the temperature of the porous hemisphere in the most heat-loaded cross section ($\eta = 0$) in the steady heat-transfer regime ($t = 200$ sec) at $(\rho v)_w(0_1) = 6$ and 12 kg/(m^2·sec) does not exceed 860 and 710 K, respectively.

Figure 5 shows the circumferential distribution of the surface temperature in the steady regime of body heating ($t = 200$ sec). The solid and dashed curves correspond to three-dimensional and two-dimensional cases at two values of the longitudinal coordinate $\bar{s}$ (solid and dashed curves 1 and 1′ correspond to $\bar{s} = 2.3$ and curves 2 and 2′ to $\bar{s} = \bar{s}_B$) for $(\rho v)_w(0_1) = 6$ and 12 kg/(m^2·sec); the equilibrium radiation temperature is plotted by dot-and-dashed curves 2 and 2′. As follows from Figs. 4 and 5, the surface temperature distribution with injection of a cooling gas is qualitatively different from the distribution $T_w(s, \eta)$ for $(\rho v)_w = 0$ for different finite values of λ_i ($i = 1, 2$). The temperature T_w on the porous part of the shell can exceed the corresponding value of T_{we}, whereas the surface temperature on the conical part, both on the leeward and windward sides, becomes significantly lower than the equilibrium radiation temperature T_{we}.

Note that the shell can be destroyed as $t \to \infty$ in the two-dimensional case at the periphery ($\bar{s} = \bar{s}_B$, $\eta = 0$), where the maximum temperature of the body is achieved (dashed curve 2 in Fig. 5), whereas the body temperature does not reach the copper melting point in the case of three-dimensional heat transfer because of significant heat overflow in the circumferential direction (solid curve 2). It follows from the analysis of Fig. 5 that the injection of a cooling gas at the stationary region of heat transfer causes a more significant stratification of the temperature curves T_w at $\eta = 0$ and 0.8π than in the heating regime at $(\rho v)_w = 0$. The

reason is the behavior of the convective heat flux from the gaseous phase q_w caused by the greater mass of the cooling gas [according to formula (1.10)], which enters the screening zone on the leeward side [dashed curve 1 for $(\rho v)_w$ in Fig. 4].

The surface temperature corresponding to $\lambda_i \to \infty$ ($i = 1, 2$) and steady three-dimensional heat transfer at $(\rho v)_w \neq 0$ (curves 1 and 2 and 1′ and 2′ in Figs. 4 and 5) decreases more than twice as compared with the data plotted in Figs. 2 and 3. The results obtained for different values $(\rho v)_w(0_1) = 0$–12 kg/(m^2·sec) confirm the conclusion that it is reasonable to use highly heat-conducting materials, which ensure intense heat removal to the region of the permeable bluntness. It follows from Figs. 4 and 5 that injection considerably decreases the maximum temperatures, but a much greater effect of decreasing the maximum temperature of the conical surface in the screening zone is exerted by using heat-conducting materials. It follows from Fig. 4 that, as the flow rate of the cooling gas increases, the temperature on the porous spherical bluntness decreases, tending to the temperature of the injected gas, which justifies the validity of the assumption [3] of using the boundary conditions of the first kind at the interface between the spherical and conical parts of the shell at intense injection from the blunted surface.

Thus, the thermophysical characteristics of the material of the exposed body have been studied in the present paper in the absence and presence of injection from a spherical blunted surface at incidence. In this case, the role of circumferential overflow of heat becomes quite significant because of the difference in heat fluxes on the leeward and windward sides. The effect of injection from the blunted surface has been analyzed for thermal conductivity varying from zero in the regime of equilibrium radiation temperature to $\lambda \to \infty$, for which the formulas for the isothermal wall temperature are derived. It has been shown that highly heat-conducting materials can be successfully used to decrease the maximum temperatures of the body due to intense heat removal to the region of a porous spherical bluntness.

This work was supported by the Russian Foundation for Fundamental Research (Grant No. 96-01-00964).

REFERENCES

1. V. A. Bashkin and S. M. Reshet'ko, "Calculation of the maximum temperature of the bluntness with account of thermal conductivity of the material," *Uch. Zap. TsAGI*, **20**, No. 5, 53–59 (1989).
2. V. I. Zinchenko, A. G. Kataev, and A. S. Yakimov, "Investigation of the temperature regimes of bodies with injection of gas from the surface," *Prikl. Mekh. Tekh. Fiz.*, No. 6, 57–64 (1992).
3. V. I. Zinchenko, V. I. Laeva, and T. S. Sandrykina, "Calculation of temperature regimes of bodies with different thermal properties," *Prikl. Mekh. Tekh. Fiz.*, **37**, No. 5, 105–114 (1996).
4. B. A. Zemlyanskii and G. N. Stepanov, "Calculation of heat transfer in a hypersonic spatial air flow around thin blunted cones," *Izv. Akad. Nauk SSSR, Mekh. Zhidk. Gaza*, No. 5, 173–177 (1981).
5. Yu. V. Polezhaev and F. B. Yurevich, *Thermal Protection* [in Russian], Énergiya, Moscow (1978).
6. V. N. Kharchenko, "Heat exchange in a hypersonic turbulent boundary layer with injection of a cooling gas through the slot," *Teplofiz. Vys. Temp.*, No. 1, 101–105 (1972).
7. V. I. Zinchenko and O. P. Fedorova, "Study of a three-dimensional turbulent boundary layer with allowance for coupled heat transfer," *Prikl. Mekh. Tekh. Fiz.*, No. 3, 118–124 (1989).
8. A. V. Bureev and V. I. Zinchenko, "Calculation of the flow field past spherically blunted cones near the plane of symmetry for various shock-layer flow regimes and injection of gas from the surface," *Prikl. Mekh. Tekh. Fiz.*, No. 6, 72–78 (1991).
9. A. A. Samarskii, *Introduction into the Theory of Difference Schemes* [in Russian], Nauka, Moscow (1971).
10. V. A. Antonov, V. D. Gol'din, and F. M. Pakhomov, *Aerodynamics of Bodies with Injection* [in Russian], Izd. Tomsk Univ., Tomsk (1990).
11. N. B. Vargraftik, *Handbook of Thermophysical Properties of Gases and Fluids* [in Russian], Fizmatgiz, Moscow (1963).